



MIT Open Access Articles

Evidence for secondary-variant genetic burden and non-random distribution across biological modules in a recessive ciliopathy

The MIT Faculty has made this article openly available. **Please share** how this access benefits you. Your story matters.

As Published	10.1038/s41588-020-0707-1
Publisher	Springer Science and Business Media LLC
Version	Original manuscript
Citable link	https://hdl.handle.net/1721.1/134169
Terms of Use	Article is made available in accordance with the publisher's policy and may be subject to US copyright law. Please refer to the publisher's site for terms of use.

Evidence for secondary-variant genetic burden and non-random distribution across biological modules in a recessive ciliopathy

Maria Kousi^{1*}, Onuralp Söylemez^{2,3,4*}, Aysegül Ozanturk¹, Sebastian Akle^{2,3}, Irwin Jungreis^{4,5}, Jean Muller^{6,7}, Christopher A. Cassa^{2,3}, Harrison Brand^{8,9}, Jill Anne Mokry¹⁰, Maxim Y. Wolf^{4,5}, Azita Sadeghpour¹, Kelsey McFadden¹, Richard A. Lewis^{10,11}, Michael E. Talkowski^{8,9,12}, H el ene Dollfus⁶, Manolis Kellis^{4,5}, Erica E. Davis¹, Shamil R. Sunyaev^{2,3,4,13}, Nicholas Katsanis^{1,#}

¹Center for Human Disease Modeling, Duke University Medical, Durham, NC USA

²Division of Genetics, Brigham and Women's Hospital, Boston, Massachusetts, USA.

³Department of Medicine, Harvard Medical School, Boston, Massachusetts, USA.

⁴Broad Institute of MIT and Harvard, Cambridge, MA

⁵MIT Computer Science and Artificial Intelligence Laboratory, Cambridge, MA

⁶Laboratoire de G en etique M edicale, Institut de G en etique M edicale d'Alsace, INSERM U1112, F ed eration de M edecine Translationnelle de Strasbourg (FMTS), Universit e de Strasbourg, Strasbourg, France

⁷Laboratoire de Diagnostic G en etique, Institut de G en etique M edicale d'Alsace (IGMA), H opitaux Universitaires de Strasbourg, 1 place de l'h opital, Strasbourg, 67091, France

⁸Molecular Neurogenetics Unit and Psychiatric and Neurodevelopmental Genetics Unit, Center for Genomic Medicine, and Department of Neurology, Massachusetts General Hospital, Boston, MA, 02114, USA

⁹Program in Population and Medical Genetics and Genomics Platform, The Broad Institute of M.I.T. and Harvard, Cambridge, MA, 02142, USA

¹⁰Department of Molecular and Human Genetics, Baylor College of Medicine, Houston, Texas, USA.

¹¹Department of Ophthalmology, Baylor College of Medicine, Houston, Texas, USA.

¹²Program in Bioinformatics and Integrative Genomics, Division of Medical Sciences, Harvard Medical School, Boston, MA, 02115, USA

¹³Department of Biomedical Informatics, Harvard Medical School, Boston, MA 02215, USA

#Correspondence to nicholas.katsanis@duke.edu

Abstract

The influence of genetic background on driver mutations is well established; however, the mechanisms by which the background interacts with Mendelian loci remains unclear. We performed a systematic secondary-variant burden analysis of two independent Bardet-Biedl syndrome (BBS) cohorts with known recessive biallelic pathogenic mutations in one of 17 BBS genes for each individual. We observed a significant enrichment of *trans*-acting rare nonsynonymous secondary variants compared to either population controls or to a cohort of individuals with a non-BBS diagnosis and recessive variants in the same gene set. Strikingly, we found a significant over-representation of secondary alleles in chaperonin-encoding genes, a finding corroborated by the observation of epistatic interactions involving this complex *in vivo*. These data indicate a complex genetic architecture for BBS that informs the biological properties of disease modules and presents a model paradigm for secondary-variant burden analysis in recessive disorders.

A persistent hurdle in interrogating the role of genetic background in human genetic disorders is our limited understanding of the properties and distribution of contributory alleles. The challenge is particularly acute in rare disorders, in which the allele frequency of both causal variants and secondary contributory alleles (i.e. alleles in loci other than the primary locus) is often low; as such population-based studies are hampered by the lack of statistical power. At the same time, transitioning from a single-gene-centric to a systems-based disease architecture defined by biological modules can inform causality, penetrance and expressivity¹.

Bardet-Biedl syndrome, a model ciliopathy, represents an opportunity to study secondary-variant burden. We and others have shown previously that BBS patients can carry secondary pathogenic variants in known BBS genes². In rare examples, such alleles can modify penetrance³, whereas, more commonly, they are thought to modulate expressivity^{4,5}. However, initial population-based studies have failed to detect an enrichment for secondary alleles in *trans* (i.e. alleles in loci other than the primary locus), suggesting that either some of the examples were exceptions, or that the incidence, distribution, and frequency of such alleles might be different than assumed *a priori*⁶. Here, we studied two BBS cohorts with unambiguous recessive pathogenic mutations in 17 established BBS genes to measure a) whether there is enrichment for secondary variants beyond the driver locus; and b) if so, whether the excess variation is concentrated within discrete disease modules or whether it is randomly distributed.

As a first step, we used targeted exon capture to sequence 102 families of Northern European⁷ ancestry (Discovery cohort), all of whom have *bona fide* pathogenic recessive mutations in one of 17 known BBS genes (*BBS1*, *BBS2*, *ARL6/BBS3*, *BBS4*, *BBS5*, *MKKS/BBS6*, *BBS7*, *TTC8/BBS8*, *BBS9*, *BBS10*, *TRIM32/BBS11*, *BBS12*, *MKS1/BBS13*, *CEP290/BBS14*, *WDPCP/BBS15*, *SDCCAG8/BBS16*, and *NPHP1*). We also sequenced an ethnically matched control cohort of 384 individuals (NEU control cohort) using the same exon capture technology (capture library, sequencing platform, and base-calling software).

Our base-calling method re-detected all 152 previously-identified pathogenic recessive mutations in our cases (50 families with compound heterozygous and 52 with homozygous mutations; **Supplementary Table S1**), indicating a negligible false negative rate. To eliminate the possibility of signal being driven by false positive events, we used Sanger sequencing to test all heterozygous burden-contributing secondary alleles at MAF<0.1% in both cases and controls. We confirmed 21 variants in the Discovery cohort and 45 in the NEU control cohort.

We then asked whether individuals with a clinical diagnosis of BBS have an increased burden of *trans* secondary variants that lie beyond the primary locus, in addition to the recessive diagnostic changes. If the recessive event at the primary locus is sufficient for disease manifestation (null hypothesis), we would expect no difference in allele burden between BBS patients and controls; however, if additional variants in *trans* with the primary locus contribute to disease, we would expect to see an enrichment of such changes in cases (burden hypothesis).

To distinguish between the two posits, we used a collapsing and combine (CMC) test⁸ of rare variants at varying in-cohort MAF cutoffs, restricting our analysis to nonsynonymous heterozygous variants beyond the primary locus. Within NEU descent individuals (n=84 cases and n=384 controls), we observed a significant enrichment for burden-contributing heterozygous *trans* variants beyond the primary driver locus (**Table 1**) in cases versus controls (CMC test $p=8 \times 10^{-3}$; OR=1.77; **Fig. 1A**) at MAF=0.1%. This result also withheld when evaluating the entire discovery cohort (n=102 cases and n=384 controls), by including 18 additional individuals of mixed European ethnicity ($p=0.008$; OR=2.12 at MAF=0.9%). Also supporting the burden hypothesis, BBS cases (n=102) showed a significant excess of singletons (alleles found just once in any cohort) versus controls in the distribution of non-synonymous variants beyond the “driver” locus ($p=0.001$; OR=2.08; **Fig. 1A** and **Table S1**). Doubletons and tripletons were found to occur equally likely between cases and controls, arguing against significant population substructure affecting the observed signal (**Table S1**).

As a further test, we next evaluated the distribution of synonymous changes across the case-control cohorts. In the absence of population structure, synonymous variants should be

distributed evenly among cases and controls; we found no significant difference in the distribution of singleton synonymous variants in the entire Discovery cohort (n=102), suggesting that population structure or another technical artifact, is not a confounder (**Table S1**). Likewise, no differences were observed in the distribution of doubletons or tripletons (**Tables S1 and S2**).

We next classified variants according to their population frequency in ExAC, reasoning that alleles that are rare in the population are more likely to represent disruptions of functional nucleotides; such an analysis is facilitated by the availability of large-scale reference datasets of human genetic variation that lend the opportunity to recognize low-frequency genetic variants (on the order of the disease prevalence), rather than being limited to the in-cohort level allelic frequency. For each BBS case with a recessive primary locus, we measured the incidence of burden alleles in the other 16 BBS genes at four ExAC-based MAF cutoffs: 1%, 0.5%, 0.1%, and 0.001%. Consistent with the CMC test, we found a significant enrichment for MAF<0.001% (“ultra-rare alleles”) in cases versus controls (2.3-fold enrichment; p=0.03; OR=2.46; **Fig. 1B**).

To confirm our findings, we assembled a replication cohort of 555 individuals composed of 89 cases with a secured molecular genetic BBS diagnosis in one of the 17 BBS genes (Replication cohort), and 466 control individuals (Exome control cohort). Using the CMC test, we once again observed a significant enrichment for burden alleles in cases versus controls (p=0.001; OR=2.11 at MAF=0.2%; **Fig. 1A**), similar to the discovery case-control dataset. Using population-based allele frequencies, we observed a significant (2.5-fold) enrichment of ultra-rare alleles (MAF<0.001%; 17 changes / 89 cases versus 35 changes / 466 controls; p=2x10⁻³, OR=2.88; **Fig. 1C**), once again similar to the Discovery cohort. Critically, testing for burden in synonymous variants showed no association (p=0.21), while testing for balancing of singletons, doubletons and tripletons was likewise bereft of evidence of population stratification bias (p=0.21 for singletons, p=0.33 for doubletons and p=0.42 for tripletons; **Table S3**); we attribute this observation to the stringent filtering of population-based MAFs (always considering the highest possible MAF) that reduced the possible inflation of population-specific alleles.

Meta-analysis of the two case cohorts (Discovery and Replication) using a Cochran-Mantel-Haenszel (CMH) procedure corroborated the enrichment of rare secondary burden alleles in BBS patients compared to controls taking into account the cohort status as a stratification variable (p<0.00001; CMH pooled OR=1.94). The enrichment withstood when considering population-based allele frequencies in BBS (29 changes / 191 cases compared to 53 changes / 850 control individuals p=4x10⁻⁴; OR=2.58; **Fig. 1D**). To obtain further evidence of the specific MAF fraction contributing to burden, we counted and subsequently normalized the number of individuals with changes in each of the four established MAF bins (1%<MAF<0.5%,

0.5%<MAF<0.1%, 0.1%<MAF<0.001%, and 0.001%<MAF<0%). Consistent with our previous observations, the signal for burden was driven exclusively by ultra-rare alleles (0.001%<MAF<0%; $p=0.0004$; OR=2.58; **Supplementary Fig. 1**).

Notably, we found that *trans*-acting secondary variants in BBS genes were more likely to disrupt strongly-conserved genomic segments in the combined BBS cases than in combined controls. We focused on Synonymous Constraint Elements (SCEs) in 29 mammalian genomes, which show protein-coding conservation and also strong non-coding constraint in synonymous positions, and thus are likely to contain overlapping functional elements, such as RNA secondary structures, or binding sites for regulatory proteins⁹. We found that secondary variants overlap SCEs for 5/76 BBS case variants (6.6%) but only for 6/371 control variants (1.6%) (hypergeometric $p=0.025$). Though these numbers are low and as such warrant caution, our data do suggest that burden-contributing variants are more likely to disrupt functional elements in BBS cases.

Next, to gain further insight into the properties that distinguish the exomes of BBS-diagnosed individuals from the exomes of individuals who carry “chance” recessive changes in BBS genes, we parsed ~10,000 exomes from the Baylor Molecular Diagnostics laboratory; we identified 50 individuals with a clinical genetic disorder other than BBS who carry homozygous rare (MAF<1%) alleles in one of the BBS genes (“non-BBS recessive” cohort). In contrast to our 191 *bona fide* BBS cases, the 50 “non-BBS recessive” individuals showed no significant burden in ultra-rare BBS alleles compared to the 850 combined control cohorts ($p=0.76$; **Fig. 1D**), consistent with the model that burden alleles contribute to the clinical manifestation of BBS.

In addition to burden alleles, we also studied differences in the primary locus mutations of BBS cases and “non-BBS recessive” individuals. Overall, 37% (71/191) of the BBS patients harbor two highly disruptive (nonsense, frameshifts, deletions, etc) mutations in the primary locus in contrast to only 2% (1/50) of the “non-BBS recessive” cases ($p=4 \times 10^{-8}$). Furthermore, for the individuals harboring at least one missense mutation in the primary locus, we attributed a weight for the impact of these nonsynonymous changes using BLOSUM (score ranges between -3 to 3, with lower scores denoting more deleterious substitutions)¹⁰. BLOSUM scores of the BBS case variants were significantly lower and thus likely more disruptive than the scores for the “non-BBS recessive” individuals, with 76% (90/118) of the *bona fide* BBS cases having a negative BLOSUM score, as opposed to only 43% (21/49) of the “non-BBS recessive” individuals ($p=4 \times 10^{-5}$; **Supplementary Figure 2**). Taken together, our data are consistent with increased mutational load both in the primary locus and in secondary *trans*-acting variants that may interact epistatically with the primary locus.

Next, we turned our attention to the question of whether the observed burden alleles are distributed randomly across the BBS genes. For this question, we tested the observed versus expected probability of an individual with a mutation in any given BBS gene to have a secondary variant in a second BBS gene. We found enrichment for a subset of genes. For example, if the primary recessive mutation occurred in *BBS5*, the secondary mutation was 13-fold more likely to occur in *BBS2* than in other BBS genes (*BBS5* → *BBS2*; $p=0.0005$). Though the small number of interactions merit caution, we observed another three such pairings to be significantly enriched: *BBS9* → *BBS10* (10-fold, $p=0.0014$); *BBS12* → *BBS4* (13-fold, $p=0.0005$); *SDCCAG8* → *BBS1* (26-fold, $p=0.0019$) (**Fig. 2A**). By contrast, *BBS1* and *BBS10*, which contribute almost 40% of the recessive drivers in our cohorts, were not enriched for secondary *trans* variants in any other specific BBS gene, suggesting that the frequency of primary drivers is not a predictor of interactions. Neither our burden observations nor the specific pairings were driven by gene size; for example, *CEP290* was the largest of the evaluated BBS loci, but showed neither a mutational enrichment nor an interaction enrichment in our analyses.

To probe deeper into the nature and distribution of interactions, we wondered whether this burden is distributed randomly across the 17-BBS gene set. We noted that primary-secondary locus interactions extend beyond the observed pairwise relationships to macromolecular complexes. We were struck that two of the four enriched interaction pairings include a chaperonin-encoding gene (*BBS10* and *BBS12*). We therefore clustered the 17 BBS genes into three previously-defined modules: the BBSome complex (*BBS1*, *BBS2*, *BBS4*, *BBS5*, *BBS7*, *TTC8* and *BBS9*)¹¹⁻¹³; the transition zone complex (*MKS1*, *CEP290*, *SDCCAG8*, and *NPHP1*)^{7,14,15}, and the chaperonin complex (*MKKS*, *BBS10* and *BBS12*)^{16,17}. For the remaining three genes/proteins (*WDPCP*, *TRIM32*, and *ARL6*), we have no information about their macromolecular complexes. Restricting ourselves to alleles at $MAF < 0.001\%$ (the bin with the most robust evidence for burden enrichment) we collapsed all alleles per module and plotted all observed interactions. We then calculated the number of interactions within and across modules (**Fig. 2B**). The distribution was non-random: across the combined BBS patient set of 191 individuals, most recessive events were contributed by chaperonin-encoding components ($p=4 \times 10^{-3}$; **Fig. 2B**), suggesting that this module potentially has the most physiologically potent interaction capability.

As part of our gene discovery work, we have tested pairs of BBS genes for their ability to interact *in vivo*. In this paradigm, we have suppressed each gene either alone or in pairs in sub-effective doses in zebrafish embryos and asked whether double suppression affected the severity of the phenotype in an additive or multiplicative fashion¹⁸. *Post-hoc* retrieval of

interaction data across 19 gene pairs revealed 13 additive and six epistatic interactions (**Fig. 2C**)^{17,19-22}. Strikingly, all six observed epistatic interactions involved one of the chaperonins, whereas none of the non-chaperonin pairings showed epistasis ($p=0.003$).

In this study, we provide direct evidence for the enrichments of ultra-rare alleles in BBS patients with diagnosed recessive mutations. The degree of enrichment (~2.5-fold) is similar in both our cohorts and is only detectable for ultra-rare alleles ($MAF < 0.001\%$), consistent with population-level selection against these mutations, and indicating that they are likely deleterious and occurring at functional positions. We suspect that this occurs because the majority of variants are likely detrimental to protein function at this MAF; the study of larger cohorts should allow for the detection of more common alleles, especially if it is coupled to rigorous functional studies to determine their effect. We also note that the non-random distribution of these variants underscores biological substructure in this module. Although we are cautious to avoid over-interpreting our data, our observations support the intuitive expectation that genetic interactions within macromolecular complexes are more likely to be additive, but interactions between complexes are more likely to be epistatic. For BBS, understanding the biochemical interplay between the chaperonin module and the BBSome will likely improve further our understanding of the role of the additional variation.

We do not know the contribution of burden to the phenotype. If the discovered variants were necessary for classically-defined penetrance, we would anticipate a substantial fraction of asymptomatic individuals with recessive BBS mutations, which is not true. At the same time, pure modifiers of expressivity would have no mechanistic reason to be enriched in our cohort, since we did not pre-select for endophenotypes. The most parsimonious explanation is that recessive mutations are necessary to cause disease but are not sufficient to meet the threshold of a clinical BBS diagnosis; that is achieved through additive or multiplicative interactions with deleterious variants in other components of the module. Our current data indicate that approximately 22% of our patients carry one or more additional ultra-rare variants at the $MAF < 0.1\%$ cutoff (at which significant enrichment for secondary *trans* variants is detected with the CMC test analysis). This is likely to be an under-estimate of burden since additional *trans* alleles are likely to be a) of higher frequency than we have statistical power to detect in this cohort; b) lie elsewhere in the known BBS genes; and c) are likely to also exist in non-BBS-causing recessive loci that are nonetheless relevant to the function of the BBS biological modules.

Finally, we emphasize the fact that studies of genetic burden in rare genetic disorders can be powered significantly by biological insight. In our datasets, had we attempted agnostic

genome-wide tests, the observed burden would have been invisible because of the size of the denominator. Focusing on comprehensive set of known disease-causing genes allows a sensible, functionally-driven hypothesis to be tested that also avoids the well-established pitfalls of single-gene candidate studies. Indeed, our findings are concordant with recent studies of other genetic disorders, including Charcot-Marie-Tooth disease²⁴ and retinitis pigmentosa²⁵. We speculate that the systematic measurement of burden of other genetically-heterogeneous disorders in which all the causal genes are considered as one “baseline” entity (essentially a functional operon) will reveal similar burden observations, which in turn can be used to understand biological and biochemical substructure.

Methods

Research participants

We assessed two cohorts of individuals who fulfilled the clinical diagnostic criteria for BBS²⁶. The Discovery cohort comprised 102 patients of northern European descent and the Replication cohort 89 unrelated individuals of mixed ethnicity, respectively (**Supplementary Table S4**). The control cohorts included 384 northern European individuals (NEU control cohort) and 466 whole exome sequenced unaffected individuals of mixed ethnicity (Exome control cohort). A cohort of 50 individuals with a non-BBS genetically identified disorder, who were harboring at least two alleles with MAF<1% in one of the 17 BBS loci evaluated, was also assembled (“non-BBS recessive” cohort). Informed consent was obtained from all controls, BBS cases, and their willing family members according to protocols approved by the Institutional Review Boards of the Duke University Medical Center, the Université de Strasbourg (“Comité Protection des Personnes” EST IV, N°DC-20142222) and the Baylor College of Medicine. We obtained peripheral whole blood samples from participants and extracted DNA according to standard methods.

Targeted exome capture and next generation sequencing

The BBS patients and controls were sequenced either by regional capture of the exons and intron-exon boundaries of 785 ciliary genes prioritized from the ciliary proteome²⁷, or by direct Sanger sequencing of each exon in a CLIA laboratory²⁸. We captured regions of interest with a custom NimbleGen targeted liquid capture (12,000 exons; 1.9 Mb of target) according to manufacturer’s instructions, pooled 23 samples/pool, and subsequently performed next-generation sequencing with an Illumina HiSeq2000 platform (paired-end 100bp reads with two pools/lane; 10 lanes total). The samples were sequenced with a mean of 110x coverage with 92% of bases achieving >20x coverage and 99% of targeted regions captured. All discovered alleles at MAF<1% were confirmed by secondary Sanger sequencing. The “non-BBS recessive” cohort was sequenced by whole exome capture methodology and underwent the same analysis as previously described²⁹.

Mutation burden analysis

We performed a unidirectional gene-based association test⁸ using the mutational target of 17 BBS genes as a single grouping unit. To assess the contribution of burden alleles beyond the primer driver locus, each BBS patient’s genotype at the respective driver locus was set to homozygous reference. Missing genotypes in both cases and controls were imputed to

reference. Restricting to nonsynonymous single nucleotide variants with high impact on protein function (missense and nonsense consequences as annotated by SnpEff v4.3)³⁰, we performed collapsing and combine (CMC) test of rare variants at various in-cohort minor allele frequency (MAF) cutoffs as well as at the optimal in-cohort frequency cutoff selected using a variable threshold (VT) approach³¹, as implemented in RVTESTS package³². To mitigate potential bias due to imperfect ethnicity matching between cases and controls, we repeated the burden analysis excluding 18 individuals with non-Northern European ancestry.

We assessed mutational burden in BBS cases, controls and the cohort of “non-BBS recessive” individuals with a known primary recessive driver gene (**Supplementary Table S4**). For inclusion, variants fulfilled the following criteria: 1) likely disruptive to protein sequence i.e. nonsynonymous, nonsense, frameshifting, *bona fide* splice sites within three base pairs of exon-intron junctions, and CNVs described previously^{19,20}; 2) ethnically-matched MAF<1% (as obtained from the ExAC browser: <http://exac.broadinstitute.org/> and/or the Greater Middle East (GME) Variome: <http://igm.ucsd.edu/gme/index.php>) and 3) restricted to the 17 BBS genes sequenced across all three cohorts. The statistical significance between control and affected individuals with variants likely contributing to burden was compared among groups (Discovery cohort vs NEU control cohort; Replication cohort vs Exome control cohort; Combined BBS cohorts (Discovery+Replication) vs Combined control cohorts (NEU control cohort+ Exome control cohort) with a two-tailed Fisher’s exact probability test.

Synonymous Constraint Elements

We searched for Synonymous Constraint Elements (SCEs) in every coding sequence in CCDS Homo Sapiens release 9 using FRESCo software³³. FRESCo analysis was performed using a window size of 9 and sequences and distances taken from the 29 mammal alignment³⁴. The resulting list of SCEs is available at

<https://data.broadinstitute.org/compbio1/SynonymousConstraintTracks/ESS.hg19.bed.gz>. We

tested each burden SNV in each individual and found the following changes to be contained in an SCE: for cases: AR201-06, BBS9: p.Ser753Phe; AR831-03, BBS4: p.Pro13Ser; KK011-04, SDCCAG8: p.Glu532Lys; Fam93_NNMR18, BBS4: p.R295Q; Fam14_AKX44, SDCCAG8: p.Q505E; for controls: 37 - 10101398_C31NDACXX-7-IDMB39, NPHP1: p.S29F; 246 - 10104594_C30WYACXX-4-IDMB66, BBS9: p.S788F; DM414-1000, NPHP1: p.M616I; DM773-1000, NPHP1: p.I45L; DM1377-1000, ARL6: p.G72R; DM1377-1001, BBS9: p.S788F.

BLOSUM scoring

BLOSUM score was calculated using the blosum62 matrix obtained from biopython version 1.58. The BLOSUM score ranges from -3 to 3 with lower numbers indicating biochemically more different pairs of amino acids and higher scores indicating more-radical amino acid changes. For BBS cases with two missense changes at the recessive locus, the change with the higher BLOSUM score was taken into consideration.

Acknowledgements

We thank the patients and their families for participating in this study, as well as their caring physicians that provided clinical information and referred the patients for diagnostic analyses. We thank Anne-Sophie Jaeger and Manuela Antin for the technical assistance. This study was supported by the NIH grants GM121317-13, HD042601, and DK072301 (N.K.). R01 HG004037 (I.J.) and GENCODE Wellcome Trust grant U41 HG007234 (I.J.). R.A.L. is a senior scientific investigator of research to prevent blindness. N.K. is a distinguished Jean and George Brumley Professor.

Author contributions

M.K., E.E.D. S.S. and N.K. designed the overall study. M.K., A.O., and K.M. performed the experimental work by genotyping and analyzing the sequencing data. O.S., S.A., C.A.C., M.K., H.R. and M.E.T., and S.S. performed the statistical analysis assessing mutational burden. I.J., M.Y.W. and M.K. performed the analyses assessing the impact of the identified changes on genomic sequence signatures. J.M., J.A.M. R.A.L. and H.D. contributed samples that were analyzed in this study. A.S. collated the genetic information of the Discovery cohort. M.K. performed the collective analysis of genetic data and modular interactions. All authors have read and commented on the manuscript that was written by N.K. and M.K.

References

1. Skafidas, E. *et al.* Predicting the diagnosis of autism spectrum disorder using gene pathway analysis. *Mol Psychiatry* **19**, 504-10 (2014).
2. Beales, P.L. *et al.* Genetic interaction of BBS1 mutations with alleles at other BBS loci can result in non-Mendelian Bardet-Biedl syndrome. *Am J Hum Genet* **72**, 1187-99 (2003).
3. Katsanis, N. *et al.* Triallelic inheritance in Bardet-Biedl syndrome, a Mendelian recessive disorder. *Science* **293**, 2256-9 (2001).
4. Badano, J.L. *et al.* Dissection of epistasis in oligogenic Bardet-Biedl syndrome. *Nature* **439**, 326-30 (2006).
5. Cardenas-Rodriguez, M. *et al.* The Bardet-Biedl syndrome-related protein CCDC28B modulates mTORC2 function and interacts with SIN1 to control cilia length independently of the mTOR complex. *Human Molecular Genetics* **22**, 4031-4042 (2013).
6. Shaheen, R. *et al.* Characterizing the morbid genome of ciliopathies. *Genome Biol* **17**, 242 (2016).
7. Otto, E.A. *et al.* Candidate exome capture identifies mutation of SDCCAG8 as the cause of a retinal-renal ciliopathy. *Nature genetics* **42**, 840-850 (2010).
8. Li, B. & Leal, S.M. Methods for detecting associations with rare variants for common diseases: application to analysis of sequence data. *Am J Hum Genet* **83**, 311-21 (2008).
9. Lin, M.F. *et al.* Locating protein-coding sequences under selection for additional, overlapping functions in 29 mammalian genomes. *Genome Res* **21**, 1916-28 (2011).
10. Henikoff, S. & Henikoff, J.G. Amino acid substitution matrices from protein blocks. *Proc Natl Acad Sci U S A* **89**, 10915-9 (1992).
11. Loktev, A.V. *et al.* A BBSome subunit links ciliogenesis, microtubule stability, and acetylation. *Dev Cell* **15**, 854-65 (2008).
12. Nachury, M.V. *et al.* A core complex of BBS proteins cooperates with the GTPase Rab8 to promote ciliary membrane biogenesis. *Cell* **129**, 1201-13 (2007).
13. Wei, Q. *et al.* The BBSome controls IFT assembly and turnaround in cilia. *Nat Cell Biol* **14**, 950-7 (2012).
14. Garcia-Gonzalo, F.R. *et al.* A transition zone complex regulates mammalian ciliogenesis and ciliary membrane composition. *Nat Genet* **43**, 776-84 (2011).
15. Seeger-Nukpezah, T. *et al.* The centrosomal kinase Plk1 localizes to the transition zone of primary cilia and induces phosphorylation of nephrocystin-1. *PLoS One* **7**, e38838 (2012).
16. Kim, J.C. *et al.* MKKS/BBS6, a divergent chaperonin-like protein linked to the obesity disorder Bardet-Biedl syndrome, is a novel centrosomal component required for cytokinesis. *J Cell Sci* **118**, 1007-20 (2005).
17. Stoetzel, C. *et al.* Identification of a novel BBS gene (BBS12) highlights the major role of a vertebrate-specific branch of chaperonin-related proteins in Bardet-Biedl syndrome. *Am J Hum Genet* **80**, 1-11 (2007).
18. Leitch, C.C. *et al.* Hypomorphic mutations in syndromic encephalocele genes are associated with Bardet-Biedl syndrome. *Nat Genet* **40**, 443-8 (2008).
19. Lindstrand, A. *et al.* Recurrent CNVs and SNVs at the NPHP1 locus contribute pathogenic alleles to Bardet-Biedl syndrome. *Am J Hum Genet* **94**, 745-54 (2014).
20. Lindstrand, A. *et al.* Copy-Number Variation Contributes to the Mutational Load of Bardet-Biedl Syndrome. *Am J Hum Genet* **99**, 318-36 (2016).
21. Stoetzel, C. *et al.* BBS10 encodes a vertebrate-specific chaperonin-like protein and is a major BBS locus. *Nat Genet* **38**, 521-4 (2006).

22. Zaghoul, N.A. *et al.* Functional analyses of variants reveal a significant role for dominant negative and common alleles in oligogenic Bardet–Biedl syndrome. *Proceedings of the National Academy of Sciences of the United States of America* **107**, 10602-10607 (2010).
23. Estrada-Cuzcano, A. *et al.* BBS1 mutations in a wide spectrum of phenotypes ranging from nonsyndromic retinitis pigmentosa to Bardet-Biedl syndrome. *Arch Ophthalmol* **130**, 1425-32 (2012).
24. Gonzaga-Jauregui, C. *et al.* Exome Sequence Analysis Suggests that Genetic Burden Contributes to Phenotypic Variability and Complex Neuropathy. *Cell Rep* **12**, 1169-83 (2015).
25. Nikopoulos, K. *et al.* Frequent variants in the Japanese population determine quasi-Mendelian inheritance of rare retinal ciliopathy. *bioRxiv* (2018).
26. Beales, P.L., Elcioglu, N., Woolf, A.S., Parker, D. & Flinter, F.A. New criteria for improved diagnosis of Bardet-Biedl syndrome: results of a population survey. *J Med Genet* **36**, 437-46 (1999).
27. Hjeij, R. *et al.* ARMC4 mutations cause primary ciliary dyskinesia with randomization of left/right body asymmetry. *Am J Hum Genet* **93**, 357-67 (2013).
28. Redin, C. *et al.* Targeted high-throughput sequencing for diagnosis of genetically heterogeneous diseases: efficient mutation detection in Bardet-Biedl and Alstrom syndromes. *J Med Genet* **49**, 502-12 (2012).
29. Yang, Y. *et al.* Clinical whole-exome sequencing for the diagnosis of mendelian disorders. *N Engl J Med* **369**, 1502-11 (2013).
30. Cingolani, P. *et al.* A program for annotating and predicting the effects of single nucleotide polymorphisms, SnpEff: SNPs in the genome of *Drosophila melanogaster* strain w1118; iso-2; iso-3. *Fly (Austin)* **6**, 80-92 (2012).
31. Price, A.L. *et al.* Pooled association tests for rare variants in exon-resequencing studies. *Am J Hum Genet* **86**, 832-8 (2010).
32. Zhan, X., Hu, Y., Li, B., Abecasis, G.R. & Liu, D.J. RVTESTS: an efficient and comprehensive tool for rare variant association analysis using sequence data. *Bioinformatics* **32**, 1423-6 (2016).
33. Sealfon, R.S. *et al.* FRESCO: finding regions of excess synonymous constraint in diverse viruses. *Genome Biol* **16**, 38 (2015).
34. Lindblad-Toh, K. *et al.* A high-resolution map of human evolutionary constraint using 29 mammals. *Nature* **478**, 476-82 (2011).

Table 1: Burden analysis for variants beyond the primary driver locus

Discovery cohort					Replication cohort				
Cases	Controls	OR ^a	P ^a	MAF cutoff ^b	Cases	Controls	OR	P	MAF cutoff
102	384	1.77	8×10^{-3}	0.9%	89	466	2.11	1×10^{-3}	0.2%
84 ^c	384	2.12	8×10^{-3}	0.1%					

^a Odds ratio (OR) and one-sided p-value computed using Fisher's Exact test at the optimal in-cohort frequency threshold ^b Optimal frequency threshold selected using a variable threshold approach to incorporate allele frequency information into burden analysis. Significance of the threshold test was evaluated using 10000 permutations at $\alpha=0.05$. ^c Subset of individuals with Northern European ancestry.

Figure legends

Figure 1. Distribution of burden-contributing variation across case and control cohorts.

(A) Collapsing and combine (CMC) test of rare non-synonymous heterozygous variants outside the primary driver locus at varying in-cohort minor allele frequency (MAF) cutoffs; (B) Values of burden-contributing variation between BBS cases of the Discovery cohort (N=102) and the cohort of Northern European controls (N=384); (C) BBS cases of the Replication cohort (N=89) and the Exome control cohort (N=466); and (D) collapsed cohorts, across four MAF bins (1%, 0.5%, 0.1% and 0.001%). (A) The Discovery case cohort shows a 2.3-fold enrichment for ultra-rare (MAF<0.001%) alleles compared to controls, (B) the Replication cohort shows a 2.5-fold enrichment of such alleles compared to the exome control cohort and (C) the BBS case meta-analysis a 2.4-fold enrichment compared to the combined control cohorts. (E) Distribution of individuals with burden-contributing alleles with MAF<1%; and (F) with MAF<0.001% in control individuals (blue bars) and BBS cases (orange bars).

Figure 2. Genetic and modular interactions in BBS cases and controls.

In each panel the primary loci are represented as circles in the top half and the loci contributing to mutational load as circles in the bottom half of each panel respectively. The size of the circles corresponds to the number of individuals carrying changes in the primary and burden contributing loci, respectively and the thickness of the lines connecting primary and burden-contributing loci corresponds to the frequency at which a genetic interaction is observed with thicker lines representing more common interactions. (A) In the meta-analysis of BBS cases *BBS1*, *BBS2*, *BBS10* and *BBS12* harbor recessive driver alleles most frequently but there is an even distribution of burden-contributing alleles across the 17 BBS loci. (B) Analysis of modules within the BBS proteome (BBSome: *BBS1*, *BBS2*, *BBS4*, *BBS5*, *BBS7*, *TTC8*, and *BBS9*; Chaperonin complex: *MKKS*, *BBS10*, and *BBS12*; Transition zone: *MKS1*, *CEP290*, *SDCCAG8*, and *NPHP1* and the three genes that belong to no defined yet module: *ARL6*; *TRIM32*; *WDPCP*) revealed that the components of the chaperonin complex are driving the majority of modular interactions in BBS. (C) Schematic showing the functional outcome (epistatic versus additive) upon suppression of select modular interactions using an *in vivo* zebrafish system. Epistatic interactions among loci are shown in red and additive genetic interactions are shown in orange.

Supplementary Fig. 1. Distribution of burden-contributing variation across case and control cohorts in each of four discrete MAF bins. (A) Values of burden-contributing variation between BBS cases of the Discovery cohort (N=102) and the cohort of Northern European controls (N=384); **(B)** BBS cases of the Replication cohort (N=89) and the Exome control cohort (N=466); **(C)** BBS cases of the meta-analysis (N=191) and the combined control cohorts (N=850); and **(D)** collapsed cohorts, across four MAF bins (1%<MAF<0.5%, 0.5%<MAF<0.1%, 0.1%<MAF<0.001%, and 0.001%<MAF<0%). **(A)** The Discovery case cohort shows a 2.3-fold enrichment for ultra-rare (0.001%<MAF<0%) alleles compared to controls, **(B)** the Replication cohort shows a 2.5-fold enrichment of such alleles compared to the exome control cohort and **(C)** the BBS case meta-analysis a 2.4-fold enrichment compared to the combined control cohorts.

Supplementary Fig. 2. Estimate of protein impact for the least disruptive of the diagnostic variants for BBS cases and non-BBS recessive individuals, with at least one missense change in the primary locus. With high BLOSUM62 scores denoting biochemically similar amino acid changes and lower scores marking radical amino acid changes, the graph shows evidence for *bona fide* BBS cases harboring more disruptive variants.

Table S1. Distribution of synonymous and non-synonymous singletons, doubletons and tripletons between cases and controls in the original discovery cohort.

		Cases (n=102)	Controls (n=384)	Shared	Odds Ratio	p-value^a
Synonymous	Singletons	11	22	n/a	1.88	0.068
	Doubletons	2	6	0	0	0.061
	Tripletons	0	0	1	n/a	1
Non-synonymous	Singletons	31	56	n/a	2.08	0.001
	Doubletons	1	6	4	1.15	0.71
	Tripletons	1	6	2	0.28	0.5

a One-tailed Binomial exact p-value.

Table S2. Distribution of synonymous and non-synonymous singletons, doubletons and tripletons between cases and controls when cases with non-Caucasian ancestry were excluded.

		Cases (n=84)	Controls (n=384)	Shared	Odds Ratio	p-value^a
Synonymous	Singletons	8	22	n/a	1.66	0.15
	Doubletons	0	6	0	0	0.12
	Tripletons	0	0	1	n/a	1
Non-synonymous	Singletons	26	61	n/a	1.95	0.004
	Doubletons	1	8	2	0.45	0.32
	Tripletons	1	6	2	0.23	0.16

a One-tailed Binomial exact p-value.

Table S3. Distribution of synonymous and non-synonymous singletons, doubletons and tripletons between cases and controls in the replication cohort.

		Cases (n=89)	Controls (n=466)	Shared	Odds Ratio	p-value^a
Synonymous	Singletons	14	55	n/a	1.33	0.21
	Doubletons	4	6	2	0.4	0.33
	Tripletons	0	4	4	0.68	0.42
Non-synonymous	Singletons	30	116	n/a	1.35	0.038
	Doubletons	4	19	4	0.47	0.11
	Tripletons	0	1	7	4.74	0.98

a One-tailed Binomial exact p-value.

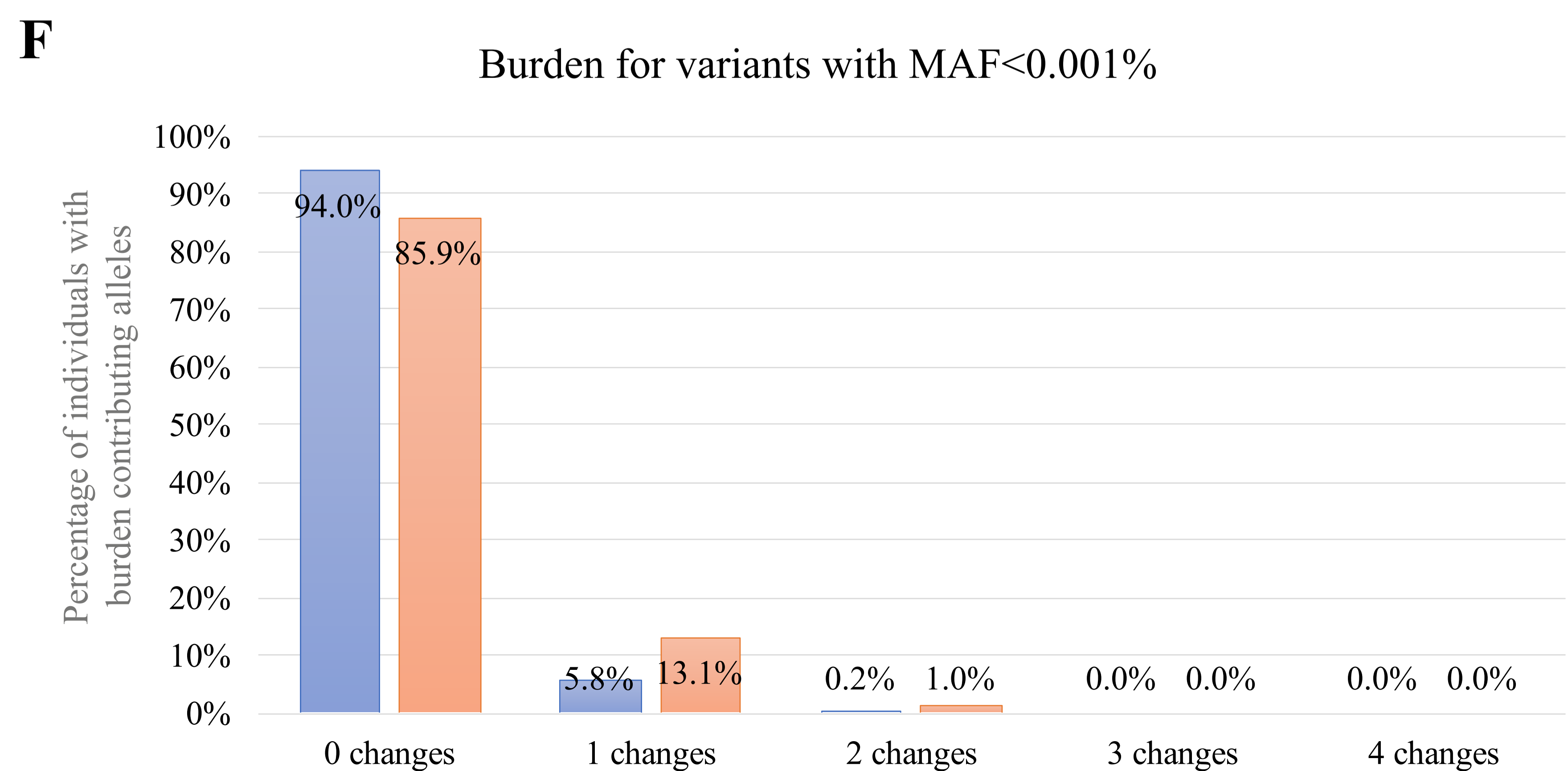
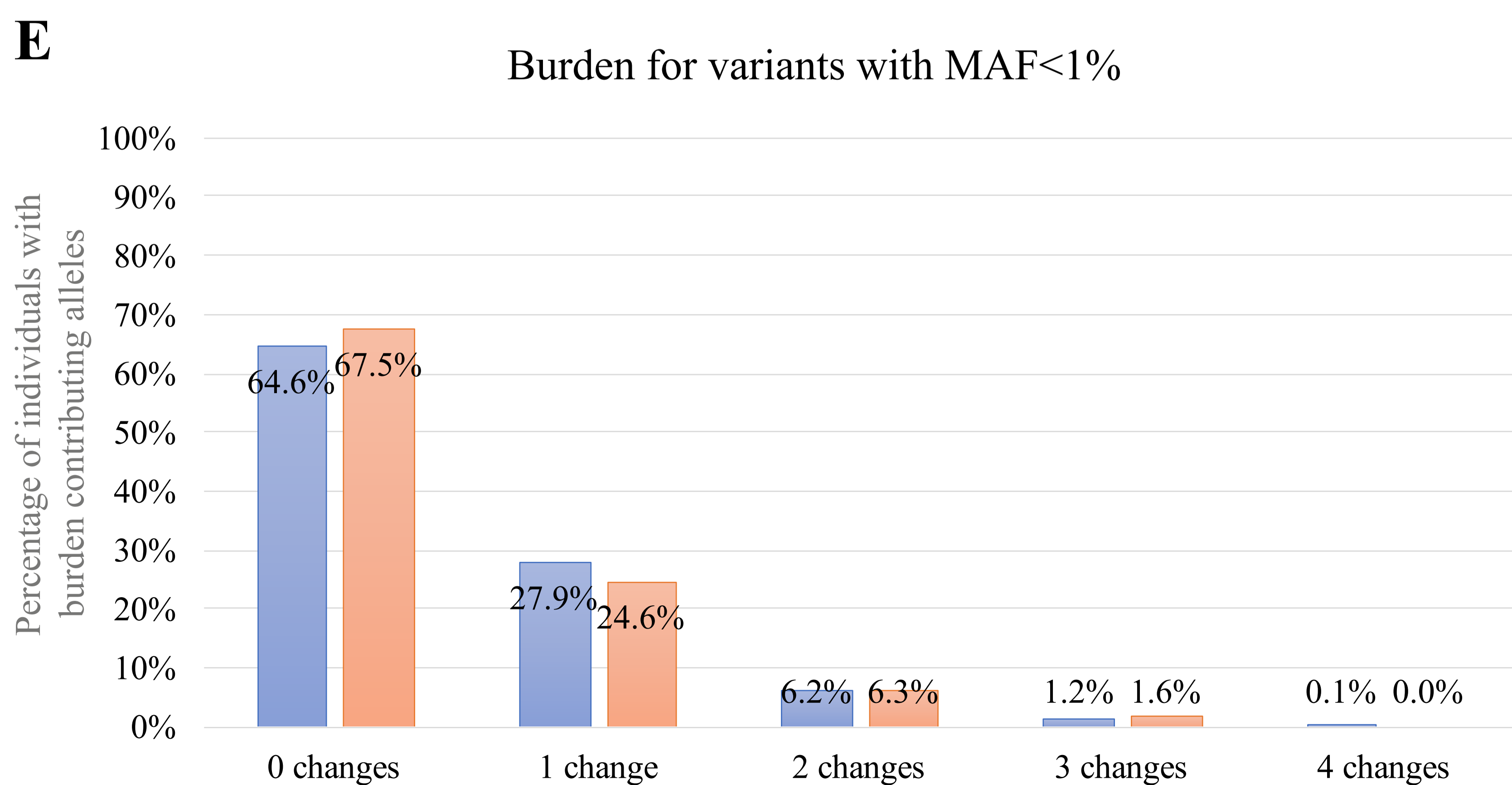
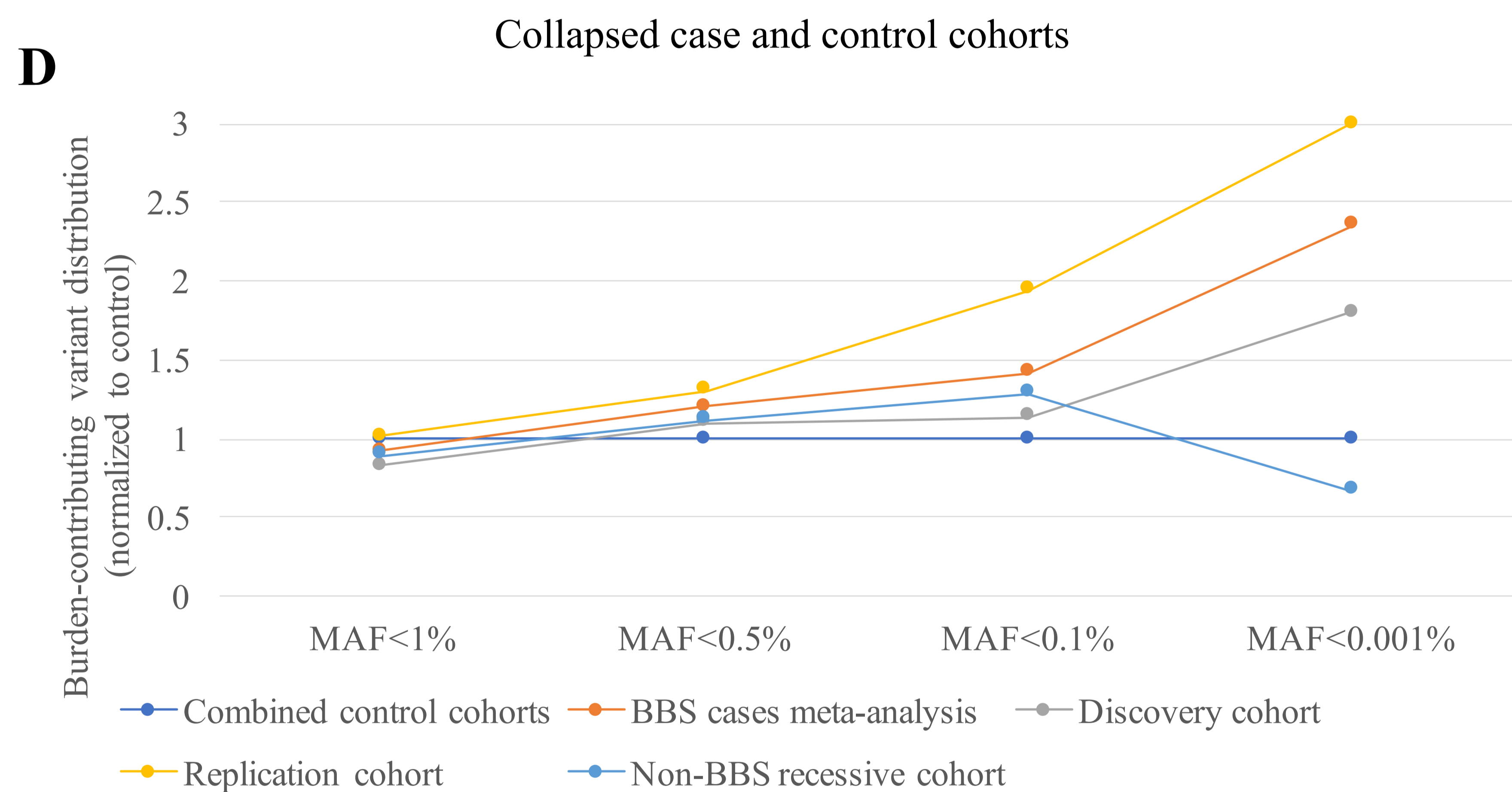
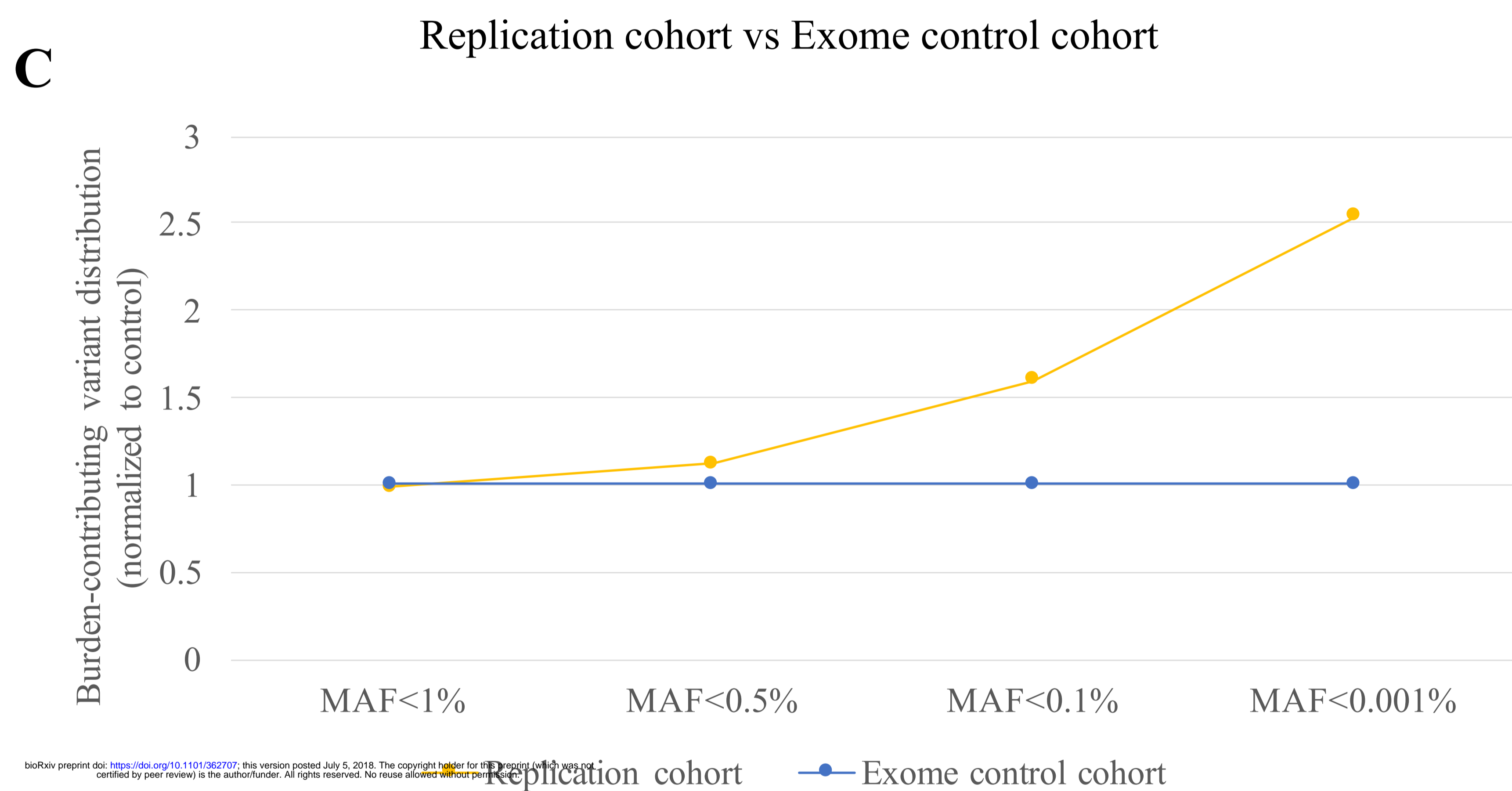
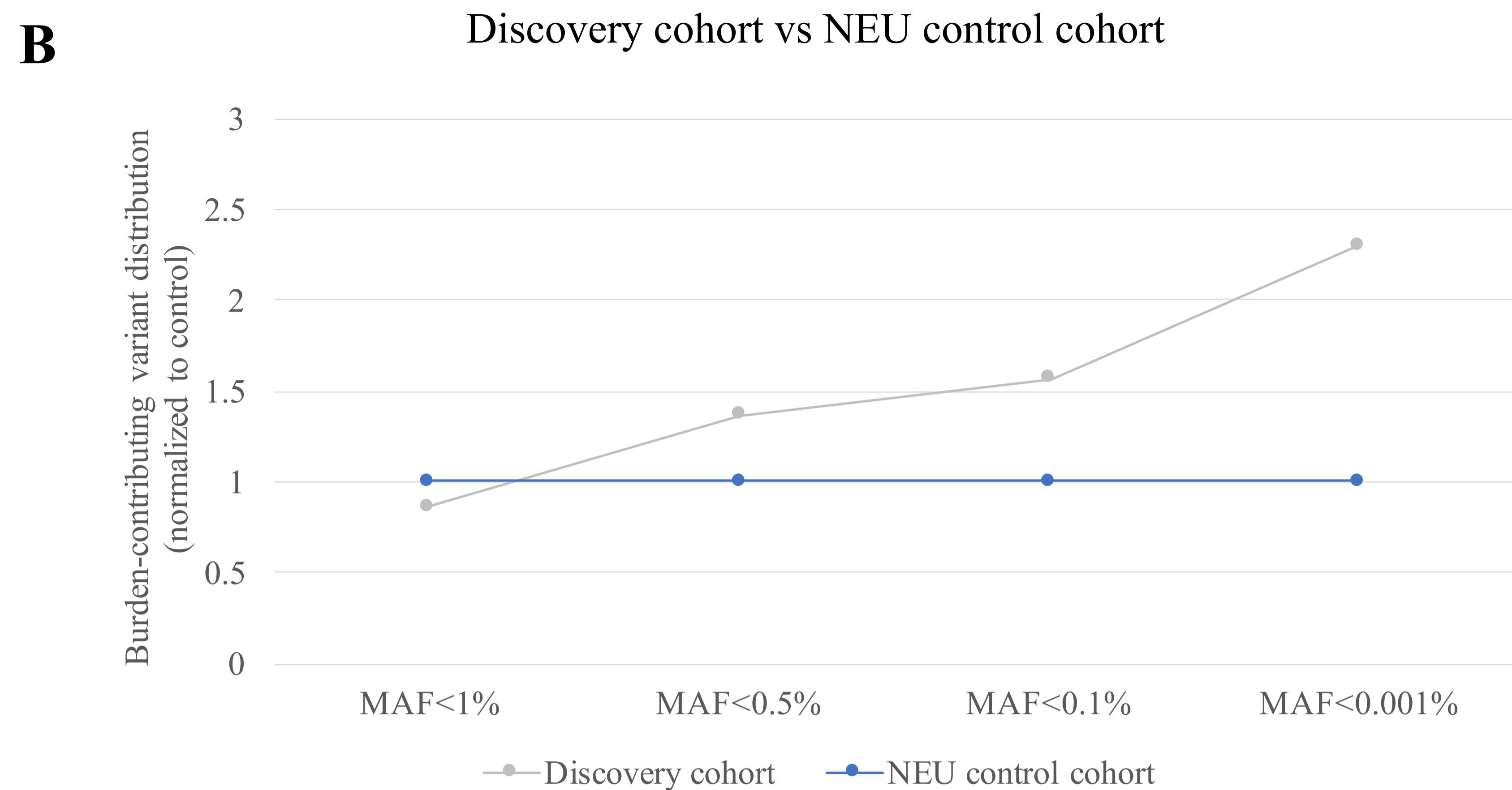
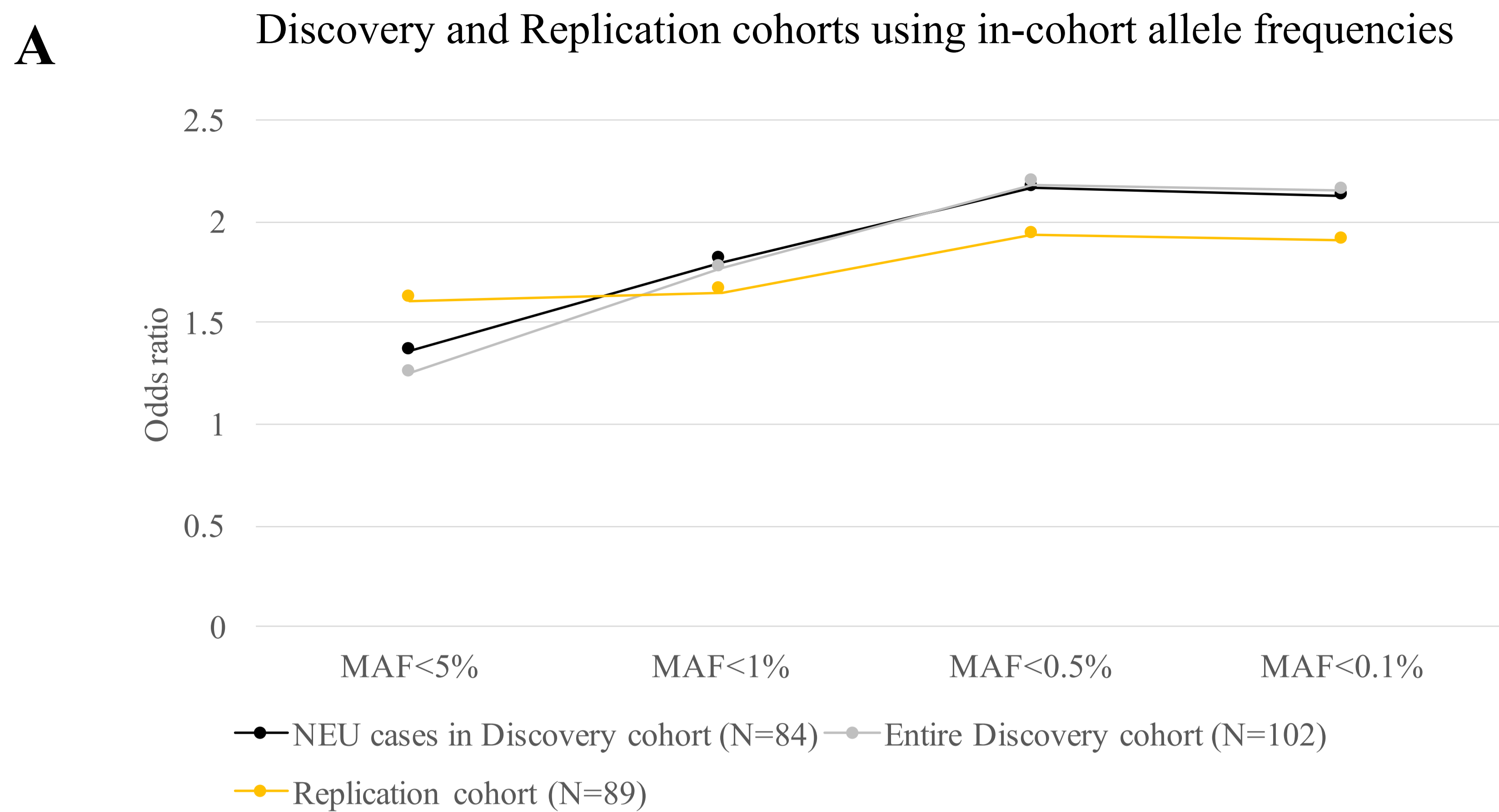
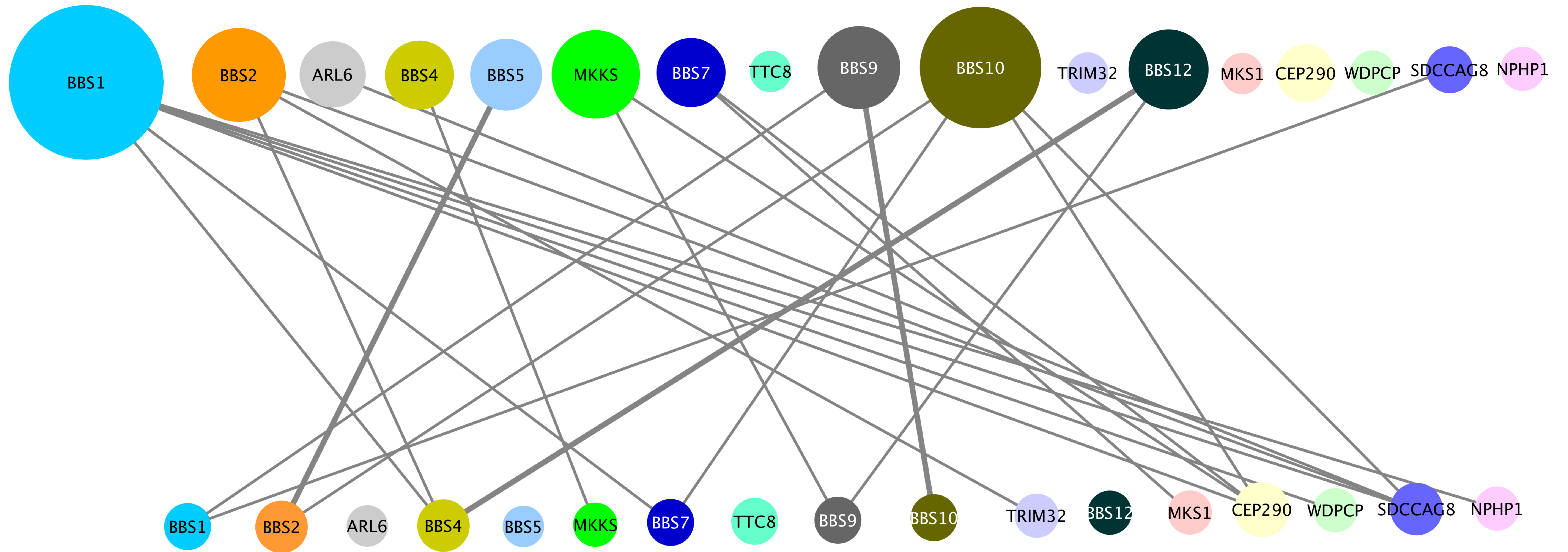
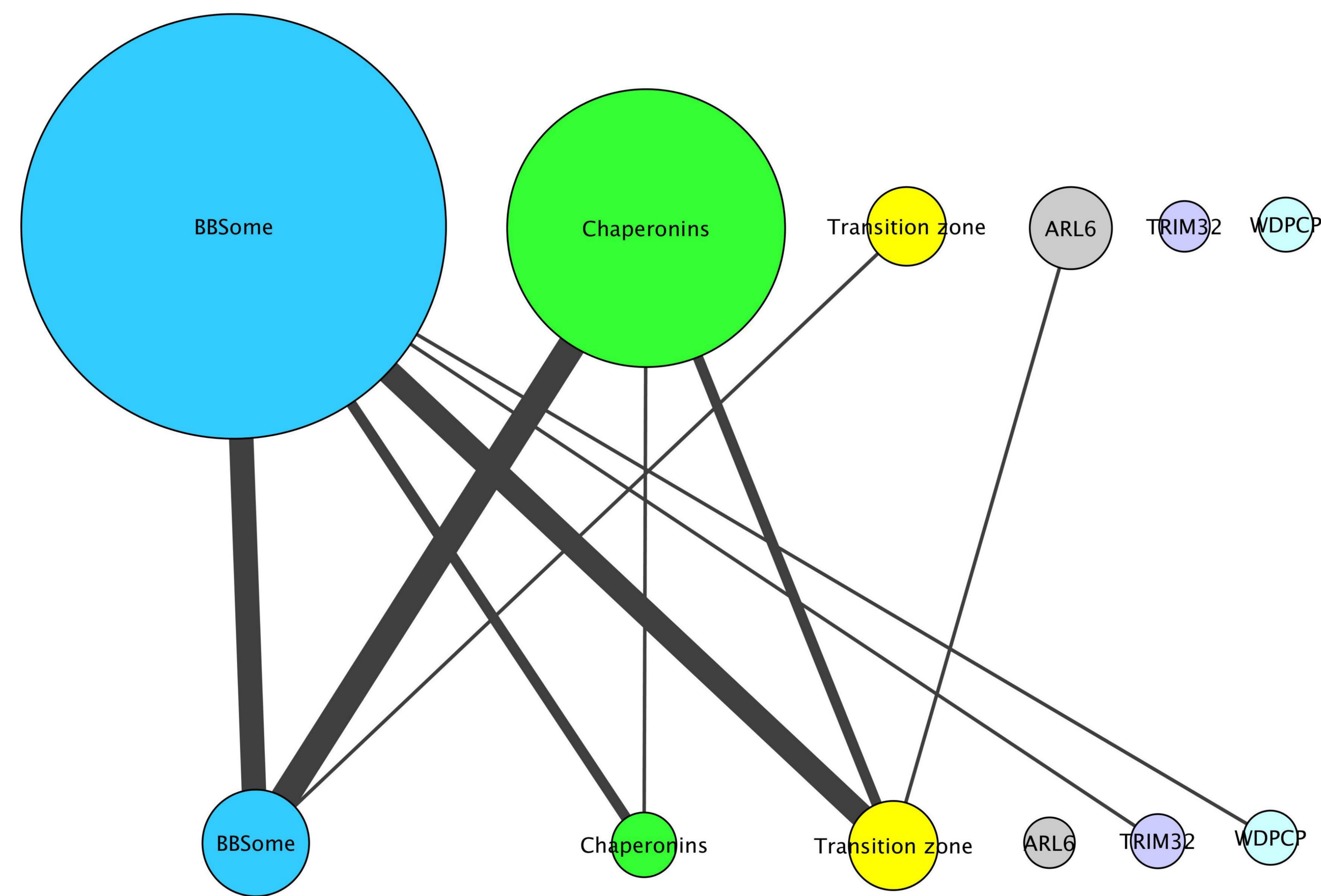
Figure 1

Figure 2

A



B



bioRxiv preprint doi: <https://doi.org/10.1101/362707>; this version posted July 5, 2018. The copyright holder for this preprint (which was not certified by peer review) is the author/funder. All rights reserved. No reuse allowed without permission.

C

	BBS1	BBS2	ARL6	BBS4	BBS5	MKKS	BBS7	TTC8	BBS9	BBS10	TRIM32	BBS12	MKS1	CEP290	WDPCP	SDCCAG8	NPHP1
BBS1		additive			additive					epistatic							additive
BBS2	additive			additive		additive											additive
ARL6																additive	
BBS4		additive				additive	additive		additive	epistatic							
BBS5	additive									epistatic							
MKKS		additive		additive						epistatic		epistatic					
BBS7				additive													additive
TTC8																	
BBS9				additive													additive
BBS10	epistatic			epistatic	epistatic	epistatic						epistatic					additive
TRIM32																	
BBS12						epistatic				epistatic							
MKS1																	
CEP290																	
WDPCP																	
SDCCAG8			additive														
NPHP1	additive	additive					additive		additive	additive							